FIRST EVIDENCE OF INCIPIENT LARGE-SCALE GRAVITATIONAL TECTONIC COLLAPSE IN SOUTH POLAR LAYERED DEPOSITS? THE CASE OF PROMETHEI LINGULA (MARS). L. Guallini[1], F. Brozzetti[2], L. Marinangeli[1], [1]IRSPS, Università d'Annunzio, V.le Pindaro 42, Pescara, Italy, guallini@irsps.unich.it; [2]Department of Earth Sciences, Università d'Annunzio, Via dei Vestini 31, Chieti Scalo, Italy.

Introduction: Deformational features have been locally identified within South Polar Layered Deposits (SPLD) by several authors [1,2,3], but in particular only in Ultimi Lobe region [4,5,6] and without a global structural survey. In the present work we focus on Promethei Lingula region (PL), where several complex deformational systems (six at least) have been found (Fig.1, [7]). Our main goal is to obtain a synoptic picture of them by 1)mapping the systems 2)carrying out a structural analysis 3)linking the observed deformations to a well defined tectonic context. New detailed modeling is partially at odd with previous work [7] and argue in favor of extensional widespread gravitational spreading, allowing us to report first possible evidences of Deep-Seated Gravitational Slope Deformations (DSGSD) observed within PLD.

Methodology: The region has been analyzed using high-resolution visible images (MRO CTX, 6.0 m/pix and HiRISE, 0.25 m/pix). Topographic basemaps are from MGS MOLA 512 pix/degree (115 m grid spacing) and from MEX HRSC DEMs (where available, 100 m - 200 m grid spacing). The datasets have been processed using the USGS ISIS 3 and georeferenced into ArcGIS 9.x. Rasters are overlaid onto HRSC DTMs in ArcScene. Structural and kinematic analysis have been done using Daisy3 (http://host.uniroma3.it/progetti/fralab/) and StereoNett 1.0.2 software.

Topographic and Structural Analysis: Deformational systems are exposed in the walls of erosional troughs walls and marginal scarps of PL (Fig.1, red triangles). Here we describe the two most representative cases. 1)*System f2* is located along a large concave sector of the PL margin and has a lateral extent of ~25 km (Fig.2a,b,c). The topography of wallrock consists on an extended bench showing a regional morphologic slope break at the elevation of ~2000 m, increasing from 5°-10° (bottom) to 15°-30° dip-angle (base). A succession of highly deformed layers is located in the lower sequence (1200m-2100m) and is characterized by spectacular wide (up to km-sized shear planes) brittle and brittle-ductile structures, cutting a section of about 900 m thick. These structures includes drag and shear folds (tangent to faults), stretched layers and boudinage. Faults and shear planes are arranged into two main cogenetic, not intersecting sets (Fig.2b: f2a, f2b) forming, at surface, a complex arcuate array. Each set appears as an en-echelon pattern of sub-parallel lineaments developing from the maximum curvature of the scarp (in map view) and laterally diverging downwards to the section base. Discontinuities cut topographic contour lines and are almost straight or slightly curved dipping conformably to the slope but at higher dip-angle (Tab.1). The top of the section is marked by three main trenches (elevation of 2200m-2300 m), several hundred meters wide, showing a maximum along-strike extent of ~6 Km. They are sub-parallel to the isohypses and cause a downslope offset of the scarp hangingwall up to ~200 m. These displacements are marked by topographic slope-breaks spacing out "terraced" surfaces. The lower portion of the wallslope shows a partial convex outward morphology (bulging), apparently due to the viscous relaxation of the layers. It's also marked by a broad and semi-continous deformed plastic (*LyP*, partially fluidified?) light-toned layer of meter-scale thickness. 2)*System f6* is exposed in a mild topographic margin indentation in Promethei Chasma (Fig.1). Its lateral extension is of ~26 km and it's characterized by a similar topographic and structural "fan-shaped" arrangement of *f2* lineaments (Fig.3a,b,c-Tab.1: f6a, f6b). The topographic slope break is at an elevation of ~2300 m, changing from 5°-10° (bottom) to 15°-20° (base) dip-angle. The more highly deformed layers are located in the top sequence (2200m-2800 m). Kilometer-scale and high dip angle faults displace a section of ~600 m thick. Faults terminate at the elevation of 2200 m. The scarp edge is marked by several wide trenches (at ~2700 m), several hundred meters wide and extending along-strike for a maximum of 12 km. The trenches follow or cross the isohypses and are well-marked by topographic steps displacing downward the slope (Fig.3c).

Family	Strike *N Azimuth*	Dip	Dip Angle *Degree*	Length *Max*
f2a	75°	345°	80°	10.5 km
f2b	131°	41°	85°	
f6a	98°	8°	80°	8.5 km
f6b	138°	48°	80°	

Tab.1: Fault planes average attitudes. Strike is measured clockwise from the North (angles<180°); dip and dip angle are derived from topographic sections or deducted from the observed relationships between fault planes and topography.

Kinematic Analysis. Both systems show comparable displacement values and complex movements consistent with a transtensional strain field (Tab.2).

Faults Systems	f2a	f2b	f6a	f6b
H-Offset (Max)	~2.5 km	~200 m	~850 m	~1.4 km
V-Offset (Max)	~200 m	~100 m	~150 m	<100 m
Main Kinematic	*SS-R* DS-N/R?	SS-L DS-N/R?	*SS-R* DS-N	*SS-L* DS-N

Tab.2. SS=Strike-Slip L(Left Lateral) R(Right Lateral), DS=Dip-Slip N(Normal) R(Reverse), in *Italic*(main component).

In general, in each system fault planes show a prevalent normal dip-slip motion in the center of the scarp, whereas a remarkable strike-slip component characterizes the scarp sides. In particular, in the W side, left-lateral faults occur, while the opposite is observed in the E side (Fig.4). Some minor fault planes strike at an acute angle (20° to 30°) with the main left-lateral systems. Taking into account their synthetic kinematic, they may be possibly interpreted as Riedel shear R1. Compressional features (reverse and transpressive faults and folded layers) locally crop out only at the base of the *f2* system, which seems to behave as a detachment level.

Discussion and Conclusions: All the observed failure systems show common topographic and structural features, referable to a similar deformational context but developed up to a different evolution grade. In our opinion, reported systems record different instances of large-scale DSGSD (fossilized?) before the final collapse. *f2* is clearly more developed (later phase, extended up to the base section) than *f6* system (earlier phase, only at the top section). Several observations support our interpretation, primarily: 1)the broad and "stair-stepped" tension fractures at the head of the scarps, 2)the "fan-shaped" setting of normal and transtensional faults as imposed by the roto-translative movements of downsloping rock volumes, 3)the foot compression of *f2*, as predicted by terrestrial analogues (thrusting, shear folding, shortened basal layers, bulging). Our observations lead us to propose the following deformational model (to be verified): 1)within chasma and troughs, gravitational ice-flow triggers extensional and lateral creep on concave-shaped scarps moving outwards the base margin, 2)scarp relaxation is likely increased in correspondence with topographic depressions at the PLD base, 3)strain give rise to several concave displacement surfaces, propagating downward, on the contrary of tectonic faults, 4)the surveyed high angle normal and transtensional faults reasonably join at depth on a weak detachment level. This gives rise to an outward sliding, which causes complex compressional structures at the base. The deformed basal layer in *f2* could be an expression of this confined compression.

At present, these systems do not seem to be active. Evidences of landslide accumulations at the scarp footwalls are absent or extremely uncertain (sublimated/eroded/never occurred?), as well as clear head-scarps. Most likely triggering factors could be warmer conditions (climatic variations) and/or impact events. Such events may also favor the partial fusion/plastification of basal levels, becoming itself a cause/consequence of the gravitational collapses.

References: [1] K.E. Herkenhoff et al. (2003) *Third Mars Polar Science Conf.*, Abstract #803.[2] K.E. Herkenhoff et al. (2008) *LPSC XXXIX*, Abstract #2361.[3] J.S. Kargel (2001), *Eos Trans. AGU*, *82*(47), F724.[4] S.M. Milkovich&J.J. Plaut (2008) *JGR*, *113*, E06007, 10.1029/2007JE002987.[5] E.J. Kolb&L. Tanaka (2006) *Mars*, *2*, 10.1555/mars.2006.0001.[6] B.M. Murray (2001) *Icarus*, *154*, 80-97, 10.1006/icar.2001.6657.[7] L. Guallini et al. (2010) *LPSC XL*, Abstract #1732.

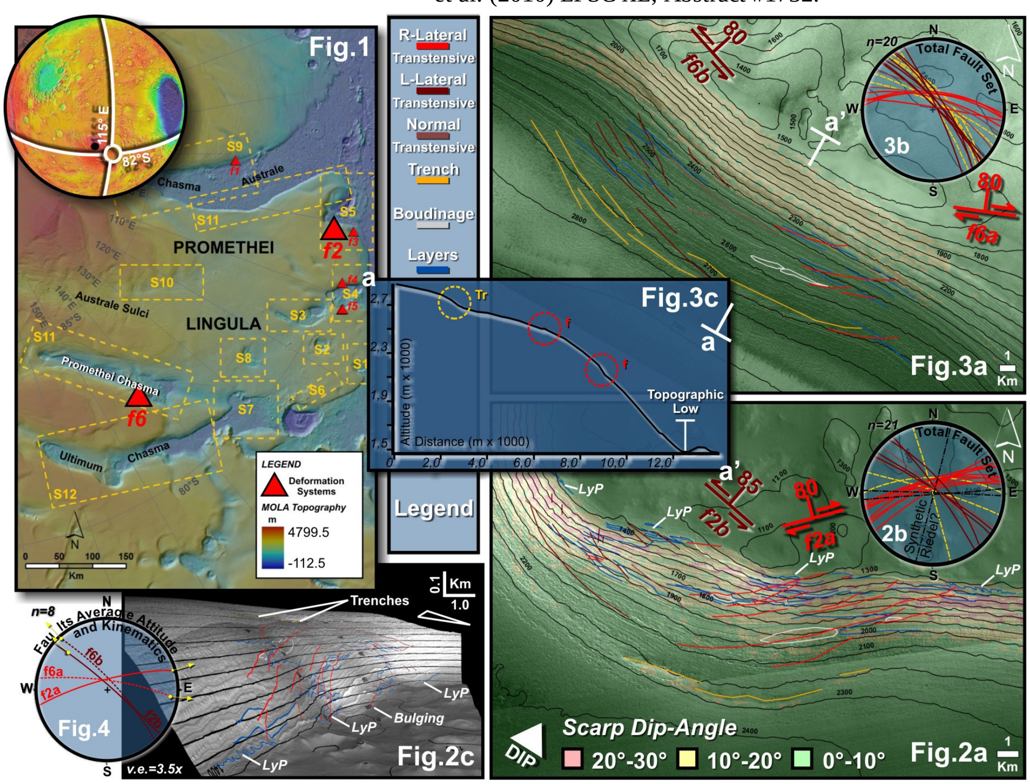

Fig.1. Location map.

Fig.2a. *f2* system. **Fig.2b.** Total *f2* fault planes set (stereographic projection, Wulff net, lower emisphere). **Fig.2c.** *f2* system, CTX on MOLA DEM.

Fig.3a. *f6* system. **Fig.3b.** Total *f6* fault planes set (stereographic projection, Wulff net, lower emisphere). **Fig.3c.** Topographic profile a-a' of *f6* system (Tr=trench f=fault).

Fig.4. Faults average attitude and kinematics (stereographic projection, Wulff net, lower emisphere, *f2* and *f6* systems).